Communications in Mathematics and Applications
Vol. 14, No. 4, pp. 1395–1403, 2023
ISSN 0975-8607 (online); 0976-5905 (print)
Published by RGN Publications
DOI: 10.26713/cma.v14i4.2576

http://www.rgnpublications.com

***Special Issue*:**
Recent Trends in Applied and Computational Mathematics
Proceedings of the Third International Conference on Recent Trends in Applied and Computational Mathematics (ICRTACM-2022)
School of Applied Sciences, Department of Mathematics,
Reva University, Bangaluru, India, 10th & 11th October, 2022
***Editors*: M. Vishu Kumar, A. Salma, B. N. Hanumagowda and U. Vijaya Chandra Kumar**

Research Article

Couple Stress Fluid Flow in A Doubly Connected Region Bounded by Elliptic Cylinders

Indira Ramarao[1], S. Pramod*[1], S. Jagadeesha[1], K. R. Rashmi[1] and K. R. Sreegowrav[2]

[1] *Department of Mathematics, Nitte Meenakshi Institute of Technology, Bengaluru, India*
[2] *Department of Mathematics, School of Applied Science, Reva University, Bengaluru, India*
***Corresponding author:** pramod.s@nmit.ac.in

Received: January 28, 2023 **Accepted:** June 3, 2023

Abstract. A doubly connected region formed by confocal elliptic cylinders is considered. The cylinder walls are assumed to be impermeable, and rigid and fully developed flow of couple-stress fluid between the cylinders is considered. Conformal mapping of the form $z = c\left(\zeta + \frac{\lambda}{\zeta}\right)$ is applied x-y plane to ξ-η plane to transform elliptical cylinders into concentric circular cylinders. The governing equations are solved analytically in ξ-η plane using the Frobenius method. The solution obtained is numerically evaluated and graphically depicted.

Keywords. Couple-stress fluid, Confocal ellipses, Doubly connected region, Conformal mapping, Frobenius method

Mathematics Subject Classification (2020). 76Rxx

1. Introduction

Some of the heat exchanges use elliptical geometries in order to transport coolants. Confocal elliptical tubes are used due to efficiency. Bordalo and Saboya [1] have conducted experimental study to analyse and establish that the pressure drop reduces in case of elliptical geometry as compared circular, Saatdjian *et al*. [11] and Mota *et al*. [8] have established the result that the performance of con focal ellipse is more optimized and better in comparison to circular cylinders. Haslam and Zamir [3] have studied pulsatile flow establishing the face that the geometry leads to Mathieu function which is complicated.

Williams *et al*. [13] have made three categories of elliptical tubes considering, two ellipses, circle in ellipse and ellipse inside a circle with free moving inner surface. Matin and Pop [6] have considered heat transfer due to natural convection in a flow of Copper Nanofluid in eccentric annulus. Zang and Li[1] understood performance of helium purification. Recently, Puranik *et al*. [9] have studied flow of Newtonian fluids under heat transfer effect in an annulus formed by con focal ellipse. They have used the approach of conformally mapping the annular region to concentric circles following Shivakumar and Ji [12]. All above studies are pertaining to Newtonian fluids. Mitsuishi and Aoyagi [7], Ebrahim *et al*. [2], He and Yang [4], Indira *et al*. [5], Rashmi and Ramarao [10] have analysed different non-Newtonian fluids flowing in annular region.

In the present study a couple-stress fluid is considered to be flowing in the annular space between elliptic cylinders which are con focal. The method used by Puranik *et al*. [9] and Shivakumar and Ji [12] is adopted for the fourth order PDE arising out of the flow. Analytical solution are obtained and graphically presented.

2. Mathematical Formulation

Annular region bounded by confocal ellipses is considered. The walls of elliptic tubes are rigid and impermeable.

The two ellipses are given by,

$$\left.\begin{aligned} &\frac{x^2}{\alpha_1^2}+\frac{y^2}{\beta_1^2}=1 \ \text{ for inner wall,}\\ &\frac{x^2}{\alpha_2^2}+\frac{y^2}{\beta_2^2}=1 \ \text{ for outer wall,}\end{aligned}\right\} \tag{1}$$

with $\alpha_1>\beta_1$ and $\alpha_2>\beta_2$ and $h=\alpha_1^2-\beta_1^2=\alpha_2^2-\beta_2^2$.

A couple stress fluid is assumed to be is shown in Figure 1 and the governing equations are given by

$$\nabla\cdot\vec{q}=0, \tag{2}$$

$$\rho\left[\frac{\partial\vec{q}}{\partial t}+(\vec{q}\cdot\nabla)\vec{q}\right]=-\nabla p+\mu\nabla^2\vec{q}-\eta_0\nabla^4\vec{q}\,. \tag{3}$$

The flow is considered to be steady and fully developed with velocity $(0,0,w)$ and under the influence of low Reynolds number. The governing equations reduce to

[1]J. Zhang and S. Li, Numerical studies of an eccentric tube-in-tube helically coiled heat exchanger for IHEP-ADS helium purification system, *arXiv:1412.8535v1* (2014), 1 – 6, DOI: 10.48550/arXiv.1412.8535.

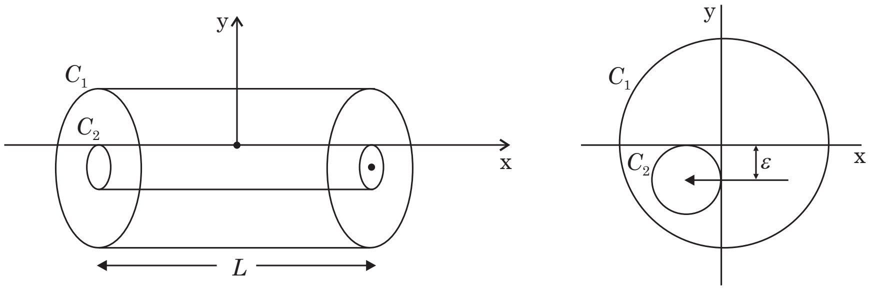

Figure 1. Physical configuration

$$\mu\Big(\frac{\partial^2}{\partial x^2}+\frac{\partial^2}{\partial y^2}\Big)w-\eta_0\Big(\frac{\partial^2}{\partial x^2}+\frac{\partial^2}{\partial y^2}\Big)^2 w=\frac{\partial p}{\partial z}. \tag{4}$$

Assuming h to be characteristic length and non dimensionalising the equation we get

$$\Big(\frac{\partial^2}{\partial x^2}+\frac{\partial^2}{\partial y^2}\Big)^2 w-\eta\Big(\frac{\partial^2}{\partial x^2}+\frac{\partial^2}{\partial y^2}\Big)w=-\frac{\eta^2}{\mu}P, \tag{5}$$

where $P=-\frac{\partial p}{\partial z}$ and η is the couple stress parameter given by $\frac{h}{\sqrt{\frac{\mu}{\eta_0}}}$.

Transforming to complex variable $Z=x+iy$ the equations take the form

$$\Big[4\frac{\partial^2}{\partial z\partial\bar{z}}\Big]^2 w-4\eta^2\frac{\partial^2 w}{\partial z\partial\bar{z}}=-\frac{\eta^2}{\mu}P.$$

Let $\frac{\partial^2 w}{\partial z\partial\bar{z}}=W$, the governing equation takes the form

$$4\frac{\partial^2 W}{\partial z\partial\bar{z}}-\eta^2 W=-\frac{\eta^2}{4\mu}P. \tag{6}$$

The above equations are subject to no slip and vanishing couple stress conditions at the boundary, i.e.,

$$w=0,\quad \frac{\partial^2 w}{\partial z\partial\bar{z}}=W=0\quad \text{on } C_1 \text{ and } C_2, \tag{7}$$

where W is real velocity and will be function of $z\bar{z}$ and $z+\bar{z}$ only.

But $W=\frac{\partial^2 w}{\partial z\partial\bar{z}}$ will be function of $z\bar{z}$. Therefore, the solution becomes using separation of variables

$$W=A_1 I_0(\eta\sqrt{z\bar{z}})+A_2 K_0(\eta\sqrt{z\bar{z}})+\frac{P}{4\mu}.$$

Integrating we get

$$w=\frac{A_1 I_0(\eta\sqrt{z\bar{z}})}{\eta^2}+\frac{A_2 K_0(\eta\sqrt{z\bar{z}})}{\eta^2}+\frac{P}{4\mu}z\bar{z}+w(z)+w(\bar{z}). \tag{8}$$

2.1 Conformal Mapping

The confocal ellipse given by (1) are mapped conformally from x-y plane to ξ-η plane using the transformation

$$z=c\Big(\zeta+\frac{\lambda}{\zeta}\Big),\quad \xi=\zeta+i\eta,\ z=x+iy. \tag{9}$$

The conformal mapping is valid whenever we have $c=\frac{\alpha_2+\beta_2}{2}>0$ and also $\lambda=\frac{\alpha_2-\beta_2}{\alpha_2+\beta_2}>0$. The confocal ellipse C_1 and C_2 are transformed to circles have radius $\zeta\bar{\zeta}=\rho=a$ and $\rho=b$ with $(a<b)$ in ξ-η plane where $a=\frac{\alpha_1+\beta_1}{2c}$, $b=\frac{\alpha_2+\beta_2}{2c}$ and $\epsilon=b-a$.

2.2 Velocity and Rate of Flow

The velocity profile is obtained by applying no-slip and vanishing couple stress at the boundaries $w=0$ and $\frac{\partial^2 w}{\partial z \partial \bar{z}}=0$ on C_1 and C_2. Transforming conformally, we get the boundary conditions in the form $w=0$ and $W=0$ on $\rho=a$ and $\rho=b$.

The solution is give in the form

$$\begin{aligned}
w=&-\frac{P}{16\eta^2}\Big[A\sum_{k=0}^{\infty}\alpha(k)\rho^{2k}\sum_{i,j}{}^kC_i\,{}^kC_{i+j}\Big(\frac{\lambda}{\rho^2}\Big)^{2(i+j)}\Big(\zeta^{2j}+\frac{\rho^{2j}}{\zeta^{2j}}\Big)\\
&+B\sum_{k=0}^{\infty}\alpha(k)\rho^{2k}\sum_{i,j}{}^kC_i\,{}^kC_{i+j}\Big(\frac{\lambda}{\rho^2}\Big)^{2(i+j)}\Big(\zeta^{2j}+\frac{\rho^{4j}}{\zeta^{2j}}\Big)\\
&\times\Big\{2\log\rho c-\chi(k+1)+\sum\frac{(-1)^s\lambda^{2s}}{s\rho^{4s}}\Big\{\zeta^{2s}+\frac{\rho^{4s}}{\zeta^{2s}}\Big\}\Big\}-\Big\{\Big(\rho^2+\frac{\lambda^2}{\rho^2}\Big)+\lambda\rho^2\Big(\zeta^2+\frac{\rho^4}{\zeta^2}\Big)\Big\}\\
&+b_0+B_1\log\rho^2\sum_j\Big(\frac{b_{2j}}{\rho^{4j}}+b_{-2j}\Big)\Big(\zeta^{2j}+\frac{\rho^{4j}}{\zeta^{2j}}\Big)\Big]\\
=&-\frac{P}{16\eta^2}[A\Gamma_1(\zeta,\bar{\zeta})+B\Gamma_2(\zeta,\bar{\zeta})-\Gamma_3(\zeta,\bar{\zeta})+b_0+B_1\log\rho^2+\Gamma_4(\zeta,\bar{\zeta})]
\end{aligned}\tag{10}$$

constants are listed in Appendix.

The rate of flow is computed using Green's theorem in complex form which is given by

$$R=\frac{1}{2i}\int_{C_1-C_2}F\,dz,\tag{11}$$

where $F=\frac{\partial w}{\partial \bar{z}}$. Substituting for velocity and applying conformal mapping

$$\begin{aligned}
R=&\frac{P}{32i\eta}\int_{C_2-C_1}\Big\{\sqrt{\frac{\bar{z}}{z}}\Big\{AI_1\Big(\frac{\eta}{2}\sqrt{z\bar{z}}\Big)+BK_1\Big(\frac{\eta}{2}\sqrt{z\bar{z}}\Big)\Big\}\Big\}z\bar{z}dz-\frac{P}{32\eta}\int_{C_2-C_1}\{\bar{z}-w'(z)\}z\bar{z}dz\\
=&\frac{P}{32\eta}\Big[A\sum_{k=0}^{\infty}\alpha_1(k)\sum_{i=0}^{\frac{k}{2}}2\,{}^kC_{2i}\Big(\rho^2+\frac{\lambda^2}{\rho^2}\Big)^{k-2i}\,{}^{2k-1}C_{i-1}\lambda^{2i}\Big(\rho^2-\frac{\lambda^2}{\rho^2}\Big)\\
&+B\sum\alpha_1(k)\{\chi(k+1)+\chi(k+2)+\log\rho c\eta\}\sum_{i=0}^{\frac{k}{2}}{}^kC_{2i}\,{}^{2i-1}C_{i-1}\Big(\rho^2+\frac{\lambda^2}{\rho^2}\Big)^k\Big]\\
&-\frac{P}{32\eta}\Big[\Big(\rho^2+\frac{\lambda^2}{\rho^2}\Big)\Big(\rho^2-\frac{\lambda^2}{\rho^2}\Big)-B\Big(\rho^2+\frac{\lambda^2}{\rho^2}\Big)+\frac{2\lambda^2}{\rho^2}b_2+4\lambda^2\rho^2b_4\Big].
\end{aligned}$$

The velocity and rate of flow are numerically evaluated and graphically depicted (see Figures 2-6).

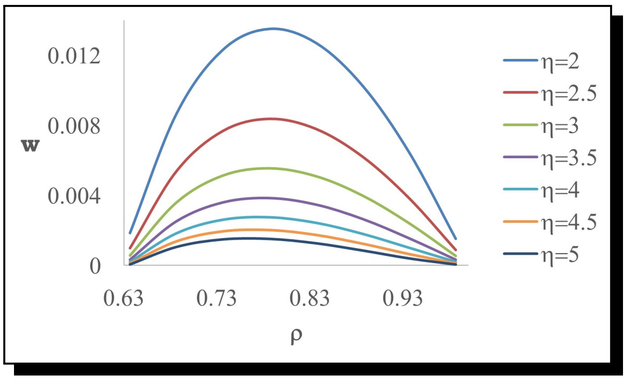

Figure 2. Plot of velocity to different couple stress parameter η for $\epsilon=0.3636$

3. Results and Discussion

An analytical study of fully developed, low Reynolds number, steady flow of couple stress fluid flowing between two confocal elliptical cylinders is considered. The distance between major and minor axes is considered as the characteristic length for the analysis. The region under consideration is conformally mapped to concentric cylinders with radius a and b.

The difference between b and a is taken as ϵ and variation due to area of cross section is analysed. The couple stress parameter inversely proportional to amount of spin and hence small values of η pertains to couple stress fluid and as $\eta \to \infty$ the fluid shows Newtonian nature.

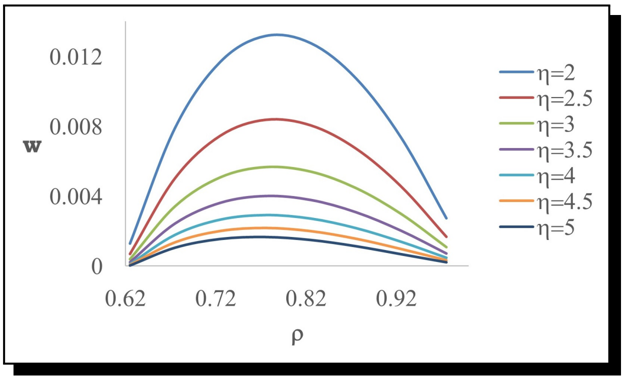

Figure 3. Plot of velocity to different couple stress parameter η for $\epsilon = 0.375$

The area of cross section depends on values of major and minor axes α_1, α_2 and β_1, β_2, but its effects is visible through radius of concentric circles b and a. Hence we have studied effect ϵ on fluid flow. The velocities profiles are plotted by assuming values of major and minor axes in x-y plane, calculating radius b and a in ξ-η plane.

The graphs from Figures 2-5 show plot of velocity along radial direction in ξ-η plane from $\rho = a$ to $\rho = b$ for different values of η and couple stress parameter η. Increase in η signifies greater area of cross-section for the flow and increase in couple stress parameter signifies loss of spin of suspended particles.

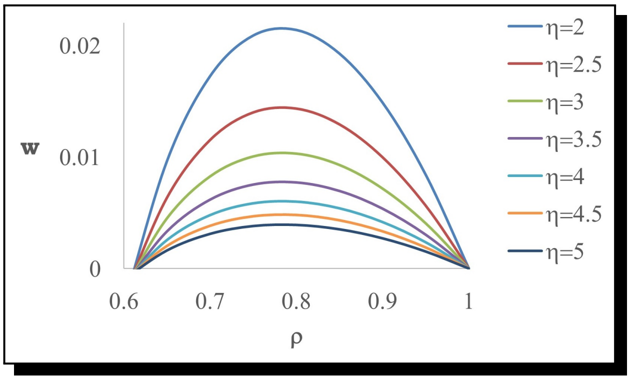

Figure 4. Plot of velocity to different couple stress parameter η for $\epsilon = 0.4$

Comparing curves for different values of η we see that velocity decreases with increasing η. The velocity shows a parabolic profile and the value of w is higher for a couple stress fluid than a Newtonian and this evident by reduction of velocity with increasing η. This signifies that the spin enhances velocity. As more area is available for flow velocity shows higher value.

For $\epsilon = 0.4$, peak of velocity is reached to 0.02 and for $\epsilon = 0.67$ it is at 0.07. As ϵ increases more fluid is accommodated and hence velocity in creases with increasing ϵ.

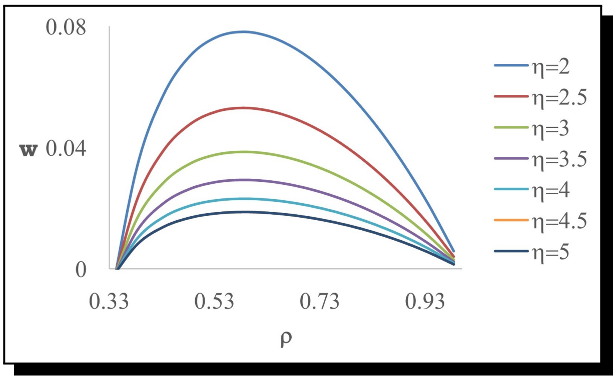

Figure 5. Plot of velocity to different couple stress parameter η for $\epsilon = 0.0.6667$

Figure 6 shows rate of flow vs couple stress parameter η for different ϵ. As ϵ increases rate of flow also increases but for increasing η, rate of flow decreases.

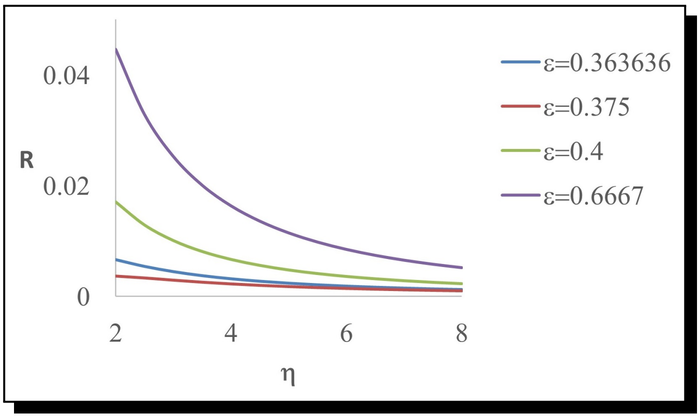

Figure 6. Plot of rate of flow for different couple stress parameter η

4. Conclusions

An attempt is made to analyse the flow of couple stress fluid flowing in an annular region created by confocal elliptical cylinders. Analytical solution is obtained using conformal mapping and series solution method. The graphs shows that couple stresses due to spin has significant effect on increase of velocity and rate of flow. As $\eta \to \infty$, the results converge for that of Newtonian fluid.

Acknowledgments

The authors extend their special thanks the management of Nitte Meenakshi Institute of Technology and Reva University, Bengaluru, India for their cooperation in bringing out of this work.

Appendix

$$\chi(k) = -0.57721566 - \sum_{i=1}^{k-1} \frac{1}{i},$$

$$\alpha(k) = \frac{(-1)^k e^{i\pi k}(\eta c)^k}{2^{2k}(k!)^2},$$

$$\alpha_1(k) = \frac{(-1)^k e^{i\pi k}(\eta c)^k}{2^{2k}k!(k+1)!},$$

$$F = \sum \alpha(k)\rho^{2k}\sum_{j=0}^{k} {}^kC_j \ {}^kC_j\left(\frac{\lambda}{\rho^2}\right)^{2j},$$

$$G = \sum \alpha(k)\rho^{2k}\sum_{j=0}^{k} {}^kC_j \ {}^kC_j\left(\frac{\lambda}{\rho^2}\right)^{2j}\{2\log(c\eta\rho)+\chi(k+1)\},$$

$$F_1 = \sum \alpha(k)\rho^{2k}\sum_{j=0}^{k} {}^kC_j \ {}^kC_{j+1}\left(\frac{\lambda}{\rho^2}\right)^{2j},$$

$$G_1 = \sum \alpha(k)\rho^{2k}\sum_{j=0}^{k} {}^kC_j \ {}^kC_{j+i}\left(\frac{\lambda}{\rho^2}\right)^{2j}\left\{2\log(c\eta\rho)+\chi(k+1)-\left(\frac{\lambda}{\rho^2}\right)^2\right\},$$

$$F_2 = \sum \alpha(k)\rho^{2k}\sum_{j=0}^{k} {}^kC_j \ {}^kC_{j+i}\left(\frac{\lambda}{\rho^2}\right)^{2(j+i)},$$

$$G_2 = \sum \alpha(k)\rho^{2k}\sum_{j=0}^{k} {}^kC_j \ {}^kC_{j+i}\left(\frac{\lambda}{\rho^2}\right)^{2i+2j}\left\{2\log(c\eta\rho)+\chi(k+1)-(-1)^k\left(\frac{\lambda}{\rho^2}\right)^{2k}\right\},$$

$$A = \frac{G(\rho_2)-G(\rho_1)}{F(\rho_2)G(\rho_1)-F(\rho_1)G(\rho_2)},$$

$$B = -\frac{F(\rho_2)-F(\rho_1)}{F(\rho_2)G(\rho_1)-F(\rho_1)G(\rho_2)},$$

$$b_0 = \rho_1^2+\frac{\lambda 2}{\rho_1^2}+4AF(\rho_1)+4BG(\rho_1)-2B\log(\rho_1),$$

$$B_1 = 4A\{F(\rho_2)-F(\rho_1)\}+4B\{G(\rho_2)-G(\rho_1)\}+\rho_2^2-\rho_1^2+\frac{\lambda^2}{\rho_1^2\rho_2^2}(\rho_1^2-\rho_2^2),$$

$$b_2 = \frac{(\rho_1\rho_2)^4}{\rho_1^4-\rho_2^4}\lambda(\rho_2^2-\rho_1^2)+4A\{F_1(\rho_2)-F_1(\rho_1)\}+4B\{G_1(\rho_2)-G_1(\rho_1)\},$$

$$b_{-2} = \lambda\rho_1^2+4AF_1(\rho_1)+4BG_1(\rho_1)-\frac{b_2}{\rho_1^4},$$

$$b_{2k} = \frac{(\rho_1\rho_2)^{4k}}{\rho_1^{4k}-\rho_2^{4k}}[4A\{F_2(\rho_2)-F_2(\rho_1)\}+4B\{G_2(\rho_2)-G_2(\rho_1)\}],$$

$$b_{-2k} = \frac{\rho_1^{4k}}{\rho_2^{4k}-\rho_1^{4k}}[4AF_2(\rho_1)+4BG_2(\rho_1)],$$

$$F_3 = \sum 2\alpha_1(k)\sum_{j=1}^{\frac{k}{2}} {}^kC_{2j} \ {}^{2j-1}C_{j-1}\left(\rho^2+\frac{\lambda^2}{\rho^2}\right)^{k-2j}\lambda^{2j}\left(\rho^2-\frac{\lambda^2}{\rho^2}\right),$$

$$G_3 = \sum 2\alpha_1(k)\sum_{j=1}^{\frac{k}{2}} {}^kC_{2j} \ {}^{2j-1}C_{j-1}\left(\rho^2+\frac{\lambda^2}{\rho^2}\right)^{(k-2j)}\lambda^{2j}\left(\rho^2-\frac{\lambda^2}{\rho^2}\right)\{2\log(c\eta\rho)-\chi(k+1)\},$$

$$H = -\left(\rho^4 - \frac{\lambda^4}{\rho^4}\right) + B_1\left(\rho_2 + \frac{\lambda^2}{\rho^2}\right) + 2\left(\frac{b_2}{\rho^2} + b_{-2}\right)\frac{\lambda}{\rho^2} + 4\left(\frac{b_4}{\rho^8} + b_{-4}\right)\lambda^2\rho^2.$$

Competing Interests

The authors declare that they have no competing interests.

Authors' Contributions

All the authors contributed significantly in writing this article. The authors read and approved the final manuscript.

References

[1] S. N. Bordalo and F. E. M. Saboya, Pressure drop coefficients for elliptic and circular sections in one, two and three-row arrangements of plate fin and tube heat exchangers, *Journal of the Brazilian Society of Mechanical Sciences* **21**(4) (1999), DOI: 10.1590/S0100-73861999000400004.

[2] N. H. Ebrahim, N. El-Khatib and M. Awang, Numerical solution of power-law fluid flow through eccentric annular geometry, *American Journal of Numerical Analysis* **1**(1) (2013), 1 – 7, DOI: 10.12691/ajna-1-1-1.

[3] M. Haslam and M. Zamir, Pulsatile flow in tubes of elliptic cross sections, *Annals of Biomedical Engineering* **26** (1998), 780 – 787, DOI: 10.1114/1.106.

[4] F.-Y. He and S.-R. Yang, Numerical simulation of unsteady flow for visco-elastic fluid in an eccentric annulus with inner rod reciprocation, *Journal of Hydrodynamics* **20** (2008), 261 – 266, DOI: 10.1016/S1001-6058(08)60055-4.

[5] R. Indira, M. Venkatachalappa and P. G. Siddeshwar, Flow of couple-stress fluid between two eccentric cylinders, *International Journal of Mathematical Sciences and Engineering Applications* **2**(IV) (2008), 253 – 261.

[6] M. H. Matin and I. Pop, Natural convection flow and heat transfer in an eccentric annulus filled by Copper nanofluid, *International Journal of Heat and Mass Transfer* **61** (2013), 353 – 364, DOI: 10.1016/j.ijheatmasstransfer.2013.01.061.

[7] N. Mitsuishi and Y. Aoyagi, Non-Newtonian fluid flow in an eccentric annulus, *Journal of Chemical Engineering of Japan* **6**(5) (1974), 402 – 408, DOI: 10.1252/JCEJ.6.402.

[8] J. P. B. Mota, I. A. A. C. Esteves, C. A. M. Portugal, J. M. S. S. Esperança and E. Saatdjian, Natural convection heat transfer in horizontal eccentric elliptic annuli containing saturated porous media, *International Journal of Heat and Mass Transfer* **43**(24) (2000), 4367 – 4379, DOI: 10.1016/S0017-9310(00)00068-5.

[9] S. M. Puranik, R. Indira and K. R. Sreegowrav, Flow and heat transfer in eccentric annulus, *Journal of Engineering Mathematics* **127** (2021), article number 21, DOI: 10.1007/s10665-021-10103-9.

[10] K. R. Rashmi and I. Ramarao, Pulsatile flow of magnetically conducting visco-elastic fluid between eccentric cylindrical tubes, *Anusandhana: Journal of Science, Engineering and Management* **7**(1) (2019), 12 – 19.

[11] E. Saatdjian, N. Midoux, M. I. G. Chassaing, J. C. Leprevost and J. C. André, Chaotic mixing and heat transfer between confocal ellipses: Experimental and numerical results, *Physics of Fluids* **8** (1996), 677 – 691, DOI: 10.1063/1.868853.

[12] P. N. Shivakumar and C. Ji, On the Poisson's equation for doubly connected regions, *Canadian Applied Mathematics* **1** (1993), 555 – 565.

[13] J. G. Williams, B. W. Turney, D. E. Moulton and S. L. Waters, Effects of geometry on resistance in elliptical pipe flows, *Journal of Fluid Mechanics* **891** (2020), A4, DOI: 10.1017/jfm.2020.121.